

Electroactive Tetrathiafulvalenyl-1,2,3-triazoles by Click Chemistry: Cu- versus Ru-Catalyzed Azide–Alkyne Cycloaddition Isomers

Thomas Biet, Thomas Cauchy, and Narcis Avarvari*^[a]

Abstract: Two series of 4- and 5-tetrathiafulvalenyl-1,2,3-triazoles, as multifunctional ligands and precursors for molecular materials, have been synthesized by copper- or ruthenium-based “click” chemistry. The solid-state structures of three ligands and two Cu^{II} complexes were determined. Large differences in the electron-donating properties between the 1,4- and 1,5-isomers were evidenced by cyclic voltammetry. Theoretical calculations support this observation and allow the assignment of the electronic transitions observed in UV/Vis spectra of the ligands.

Keywords: click chemistry • coordination chemistry • crystal structures • nitrogen heterocycles • tetrathiafulvalene

Introduction

Attachment of tetrathiafulvalene (TTF) units, well-known electroactive compounds extensively used in diverse fields of applications,^[1] to various ligands constitutes one of the privileged strategies to access valuable precursors for molecular materials.^[2] Indeed, the preparation of functional materials, in which combination of properties, such as conductivity, magnetism, luminescence, chirality, sensing, and so forth, has been achieved^[3] by starting from TTF-based ligands and -derived metal complexes, represents one of the major research direction in TTF field within the last decade.^[2] Although six-membered-ring nitrogen heterocycles, for example, pyridines, bipyridines, pyrimidines, and so forth, have been widely employed in such electroactive ligands and complexes,^[2,4] five-membered rings have been comparatively much less investigated,^[2] and especially those containing at least two nitrogen atoms. For example, two series of TTF-pyrazoles with Re^{III}^[5] and Fe^{III}^[6] complexes, respectively, have been recently described, and also two families of TTF-imidazoles, used either in conducting charge-transfer salts^[7] or as donor/acceptor compounds with tunable intramolecular charge transfer.^[8] Note that in all but one case,^[7] the TTF unit and the ligands were spaced by variable lengths linkers, and thus were not directly attached.

With the emergence and rapid widespread synthetic use of click-chemistry methods in the last decade,^[9] a few examples of TTF derivatives containing 1,2,3-triazole units have

been prepared (1,4-isomers) by using Cu-catalyzed azide–alkyne cycloaddition (CuAAC).^[10] Although the main goal of these studies was to connect the TTF unit to other moieties through the triazole linker,^[11] its propensity as a ligand has not yet been exploited. On the other hand, the complementary strategy, that is, Ru-catalyzed azide–alkyne cycloaddition (RuAAC),^[12] which gives rise to 1,5-isomers, has never been reported so far in the case of TTF–triazole derivatives. It is worth noting that 1,2,3-triazole heterocycles, besides their well-known chemical stability, aromatic character, large dipole moment (4.8–5.6 Debye), and hydrogen-bond accepting ability,^[13] proved to be not only efficient ligands for spin-crossover Fe^{II} complexes^[14] and other transition metals,^[15] although their coordination chemistry is relatively unexplored especially for the monotriazoles, but also offer an useful structural motif in peptidomimetic research^[16] and for the structure of chemical sensors.^[17] We therefore decided to directly attach a 1,2,3-triazole motif to a TTF unit to take advantage of their individual features into a multifunctional precursor for organic conductors and electroactive metal complexes. We report herein the click synthesis, solid-state structures, and properties of an unprecedented family of TTF–1,2,3-triazoles containing both 1,4- and 1,5-isomers together with Cu^{II} complexes of the latter.

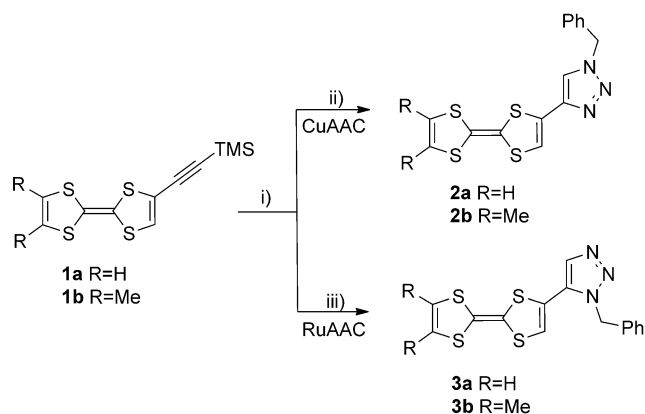
Results and Discussion

Synthesis and solid-state structures of the TTF–triazoles:

For the click reactions, TTF- or *ortho*-dimethyl-TTF-trimethylsilylethynyl derivatives **1a** and **1b**, prepared according to standard procedures (**1b** was not previously described), were first deprotected and then engaged in metal-catalyzed dipolar cycloaddition reactions to give 4-TTF–1,2,3-triazoles **2a,b** and 5-TTF–triazoles **3a,b** (Scheme 1). The conditions chosen for the CuAAC reaction used CuI as the Cu^I source^[18] because the use of the classic CuSO₄/ascorbate system proved to promote the oxidation of TTF, whereas

[a] T. Biet, Dr. T. Cauchy, Dr. N. Avarvari
LUNAM Université
Université d'Angers, CNRS UMR 6200
Laboratoire MOLTECH-Anjou
2 bd Lavoisier, 49045 Angers (France)
Fax: (+33) 02-41-73-54-05
E-mail: narcis.avarvari@univ-angers.fr

Supporting information for this article is available on the WWW under <http://dx.doi.org/10.1002/chem.201201905>.



Scheme 1. Synthesis of 4-TTF-1,2,3-triazoles **2** and 5-TTF-1,2,3-triazoles **3**. Reaction conditions: i) $(n\text{Bu})_4\text{NF}$, THF/MeOH (1:1); ii) CuI, PhCH_2N_3 , $\text{CHCl}_3/\text{DIPEA}$ (1:1), 70 °C; iii) $[\text{RuCp}^*\text{Cl}(\text{PPh}_3)_2]$, PhCH_2N_3 , THF, 65 °C. $\text{Cp}^* = 1,2,3,4,5$ -pentamethylcyclopentadienyl, DIPEA = *N,N*-diisopropylethylamine.

the standard catalyst $[\text{RuCp}^*\text{Cl}(\text{PPh}_3)_2]$ gave satisfactory results for the preparation of **3a,b**.^[19]

The four ligands were isolated in moderate (**2a,b**) and good (**3a,b**) yields as air-stable yellow–orange solids after chromatographic workup, although solutions of **2a,b** proved to be more air sensitive than those of **3a,b**. Accordingly, the comparatively lower yields obtained for the 1,4-isomers can be explained by the partial oxidation of **2a,b** during purification. Besides the usual spectroscopic characterization, suitable single crystals for X-ray analysis were obtained for **2a**, **3a**, and **3b**, whereas the crystals of **2b** were of poorer quality. Compounds **2a** and **3b** crystallize in the triclinic space group *P*-1, whereas **3a** crystallizes in the orthorhombic space group *Pcab*, all of them with one independent molecule in the asymmetric unit. It is worth noting the quasiplanarity between the triazole cycle and the TTF unit, with dihedral angles of 4.3 and 4.4° for **2a** and **3a**, respectively (Figure 1), thus suggesting some conjugation between the two moieties.

The bond lengths and angles for **2a** and **3a** are in the usual range for neutral TTF compounds, as shown by the values of the central C3=C4 bonds of 1.335(3) and 1.338(4) Å for **2a** and **3a**, respectively, and also by the averages of the internal C–S bonds of 1.760 and 1.757 Å for **2a** and **3a**, respectively. In the case of the dimethyl-TTF derivative **3b**, the dihedral angle TTF...triazole amounts to 6.0°, whereas the lengths of the central C3=C4 double bond (1.350(5) Å) is in the normal range for neutral TTF compounds (Figure 2).

At the supramolecular level, several short S...S intermolecular contacts are established especially in the packing of **2a**, in which the formation of head-to-tail dimers occurs in the *bc* plane (see Figure 3 and the Supporting Information). These dimers interact laterally along the *a* direction through S...S contacts of 3.69 and 3.73 Å. In the packing of **3a** (see the Supporting Information), the shortest S...S intermolecular contacts range between 3.84 and 3.93 Å, whereas the

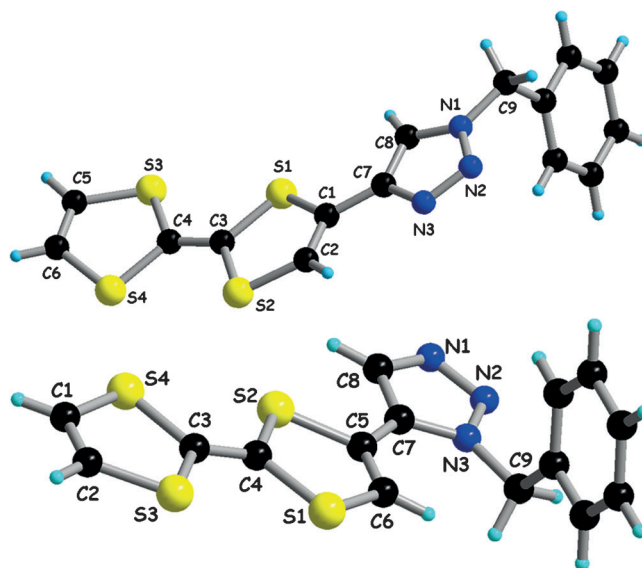


Figure 1. Molecular structures of **2a** (top) and **3a** (bottom) with the numbering scheme.

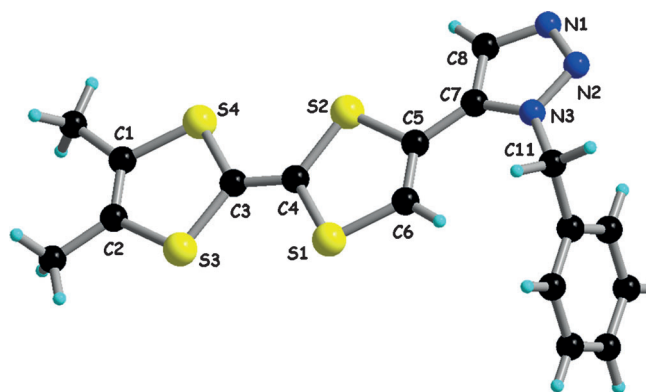


Figure 2. Molecular structure of **3b** with the numbering scheme.

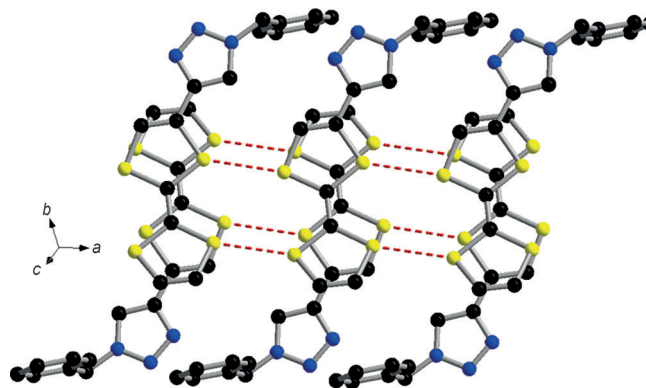


Figure 3. Packing diagram for **2a**. Intermolecular S...S contacts [Å]: S3-S4: 3.69, S3-S2: 3.92, S3-S1: 3.88, S1-S2: 3.73, S1-S4: 3.94. Highlighted: S3-S4 and S1-S2.

donors **3b** form also centrosymmetric dimers, as do **2a**, and establish short lateral S...S contacts of 3.75 Å (see the Supporting Information).

Electrochemistry and UV/Vis spectroscopy: Cyclic voltammetry (CV) measurements show reversible two one-electron oxidation processes for the four ligands, which correspond to the generation of radical cations, and then dications. The main peculiarity of the CV measurements of these ligands is the more facile oxidation of the 1,4- isomers **2a,b** with respect to the 1,5-isomers **3a,b**, as shown by $\Delta E_{1/2}^1 = 0.1$ V between **2a** and **3a** and $\Delta E_{1/2}^1 = 0.13$ V between **2b** and **3b** (Table 1). This feature suggests that the

Table 1. Redox potentials (V vs SCE) of compounds **2–4** in $\text{CH}_2\text{Cl}_2/\text{CH}_3\text{CN}$.

Compound	$E_{1/2}^{\text{ox1}}$	$E_{1/2}^{\text{ox2}}$
2a	0.39	0.83
2b	0.31	0.74
3a	0.49	0.90
3b	0.44	0.85
4a	0.28	0.68
4b	0.23	0.63

HOMO of the 1,4-isomers is comparatively higher in energy than that of the 1,5-isomers (see the theoretical calculations). Moreover, the attachment of the triazole ring on TTF as a 1,4-isomer seems to provide a slight electron-density enrichment of TTF, very likely thanks to the possible conjugation with the sp^3 N atom of the triazole ring. Note also that the dimethyl-TTF derivatives **2b** and **3b**, which are more electron rich due to the lateral methyl groups, oxidize at lower potentials than their TTF counterparts **2a** and **3a**, respectively.

Another interesting feature of this family of compounds concerns the possible charge transfer from the TTF unit to the triazole cycle. The UV/Vis spectroscopic study of the ligands shows, in all the cases, the existence of relatively large absorption bands centered at $\lambda_{\text{max}} = 388\text{--}394$ nm, with extinction coefficients between $\epsilon = 2870$ and $1760\text{ M}^{-1}\text{ cm}^{-1}$ for **2a** and **3b**, respectively (see the Supporting Information). Furthermore, the absorption bands that appear at higher energy ($\lambda_{\text{max}} = 250\text{--}350$ nm), with ϵ values on the order of $1.4 \times 10^3\text{--}1.7 \times 10^4\text{ M}^{-1}\text{ cm}^{-1}$ can be ascribed to the TTF unit^[20] and $\pi\text{--}\pi^*$ transitions of the triazole ring.

Theoretical calculations: To assign the corresponding transitions, and also to understand the better electron-donating properties of the 1,4-isomers relative to the 1,5-isomers and thus the higher stability of the latter, theoretical calculations at the DFT level were performed on the four ligands. The optimized geometries were in good agreement with those determined by X-ray diffraction studies (see Table S6 in the Supporting Information), with the exception of the dihedral angle TTF \cdots triazole in **3a,b**, which converged to a value of around 32° to accommodate an intramolecular (CH)_{TTF} \cdots Ph interaction, thus suggesting that the experimental value is determined by the solid-state packing. The analysis of the frontier orbitals shows that both the HOMO and LUMO are of the π -type, with the HOMO based exclusively on the TTF unit, whereas the LUMO has a mixed triazole/

TTF character, with the participation of the triazole ring being more important for the 1,5-isomers (around 35%) than for the 1,4-isomers (28 and 19% for **2a** and **2b**, respectively; see Figure 4 and Tables S7 and S8 in the Supporting Information).

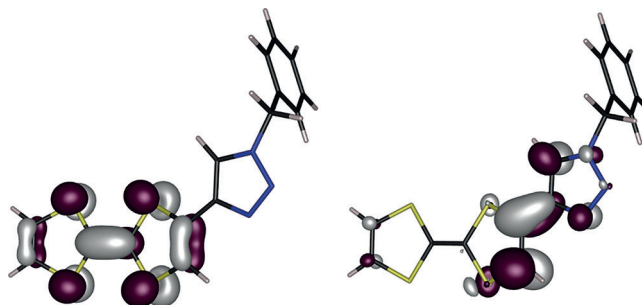


Figure 4. HOMO (left) and LUMO (right) for **2a** with an isovalue of 0.05.

An interesting feature concerns the relative positions of the HOMOs, that is, -4.89 , -4.77 , -5.13 , and -5.01 eV for **2a,b** and **3a,b**, respectively, thus clearly indicating that the 1,4-isomers **2a,b** are more electron donating than the 1,5-isomers **3a,b**, which supports the electrochemical data (see above). This difference is likely related to the position of the sp^3 N π donor atom (N1 and N3 for **2a** and **3a**, respectively; Figure 1) within the 1,3-diene system $(\text{C}=\text{C})_{\text{TTF}}\text{--C}=\text{C})_{\text{triazole}}$, that is, in the terminal position for the 1,4-isomers, which thus has an electron-enriching effect on the $(\text{C}=\text{C})_{\text{TTF}}$ group due to conjugation. However, in the 1,5-isomers this N atom is bound to the internal sp^2 C atom of the diene system, hence the donating effect is mainly felt by the $(\text{C}=\text{C})_{\text{triazole}}$ group. Note however that, very likely, a part of the π electron density of the sp^3 N atom is also delocalized over the neighboring N=N unit. Furthermore, time-dependent DFT (TD DFT) calculations, performed on the optimized geometries with the same functional, allow the assignment of the UV/Vis absorption bands (see Tables S9–12 in the Supporting Information). Accordingly, the low-energy bands calculated at $\lambda_{\text{max}} = 412$, 410, 432, and 434 nm for **2a,b** and **3a,b**, respectively, in agreement with the experimental values (see Figure 5 and the Supporting Information), correspond mainly to HOMO \rightarrow LUMO transitions and thus can be partially regarded as charge transfer from TTF to triazole, when considering the nature of the frontier orbitals.

Also, the computed relative intensities for these low-energy bands, deduced from the oscillator strength values, well reproduce the experimental ones and show that the charge transfer is slightly more favorable for the 1,4-isomers **2a,b**, probably because of the better conjugation.

Copper (II) complexes 4a,b: As mentioned above, the coordination chemistry of 1,2,3-triazoles as monodentate ligands is relatively underexplored and restrained to only a few metal centers, such as Pd^{II} , Pt^{II} , and Ag^{I} .^[15] Moderate heating of solutions of ligands **3a,b** in hexane/ CH_2Cl_2 and the Cu^{II} precursor $[\text{Cu}(\text{hfac})_2] \cdot x\text{H}_2\text{O}$ (hfac = hexafluoroace-

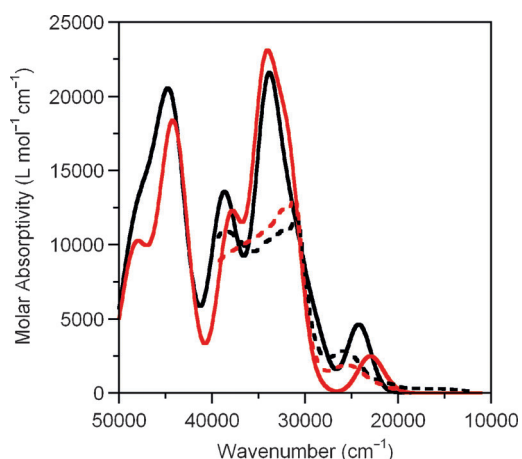


Figure 5. Experimental (dashed lines) and theoretical (solid lines) absorption spectra of **2a** (black) and **3a** (red).

tylacetate) in a 2:1 ratio, followed by the slow evaporation of the solvents, affords complexes **4a,b**, formulated as $[\text{Cu}(\text{hfac})_2(\mathbf{3})_2]$, as yellow crystalline solids. Complex **4b** (the overall quality of the structure of **4b** is superior to that of **4a**; see the Supporting Information) crystallizes in the triclinic system and space group $P\bar{1}$, with one independent half molecule in the asymmetric unit and the metal ion located on an inversion center. As generally observed in other complexes, it is the N3 atom that acts as the ligand (N1 in Figure 6). The triazole rings are now twisted by 46° with re-

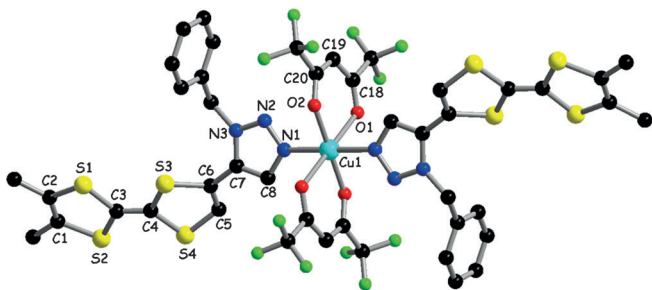


Figure 6. Molecular structure of **4b** with the numbering scheme. Hydrogen atoms have been omitted.

spect to the TTF units and coordinate the metal center *trans* to each other. The observed twist between the TTF and triazoles is very likely due to the establishment of unconventional intermolecular $\text{CH}_{(\text{TTF})} \cdots \text{O}_{(\text{hfac})}$ hydrogen bonds (see Figure S10 in the Supporting Information) as attested by the short distance $\text{H5} \cdots \text{O1}(1+x, y, z)$ of 2.68 Å. Moreover, an intramolecular $\text{CH}_{(\text{triazole})} \cdots \text{O}_{(\text{hfac})}$ interaction can be disclosed, when considering the short distance $\text{H8} \cdots \text{O2}$ of 2.69 Å. Note that, when relative to the structures of the ligands, the mutual conformation between the TTF and triazole units is now *s-cis*, when considering the relative orientation of the double bonds $\text{C5}=\text{C6}$ and $\text{C7}=\text{C8}$ with respect to the single bond $\text{C6}-\text{C7}$. However, in solution it is conceivable that the

two units can adopt a coplanar arrangement, in which establishment of intramolecular hydrogen bonding might occur, especially of the $\text{CH}_{(\text{triazole})} \cdots \text{O}_{(\text{hfac})}$ type, with regard to the proximity of the triazole and hfac groups.

The Cu^{II} center lies in a slightly distorted-octahedral coordination geometry, as shown by the angles about the metal center, which are close to 90° , whereas the $\text{Cu}-\text{O1}$ bonds (2.298(3) Å) are significantly longer than the $\text{Cu}-\text{O2}$ and $\text{Cu}-\text{N3}$ bonds (1.977(2) and 2.013(3) Å, respectively). The central $\text{C3}=\text{C4}$ bond length (1.339(5) Å) clearly indicates that the TTF unit is neutral. At the supramolecular level, the formation of dimers in the *bc* plane through the establishment of $\text{S} \cdots \text{S}$ intermolecular contacts of 3.87–3.89 Å is observed (Figure 7), whereas the shortest $\text{Cu} \cdots \text{Cu}$ distance amounts to 7.25 Å. Note that shorter lateral $\text{S2} \cdots \text{S2}$ contacts of 3.54 Å are established between the dimers along the *a* direction.

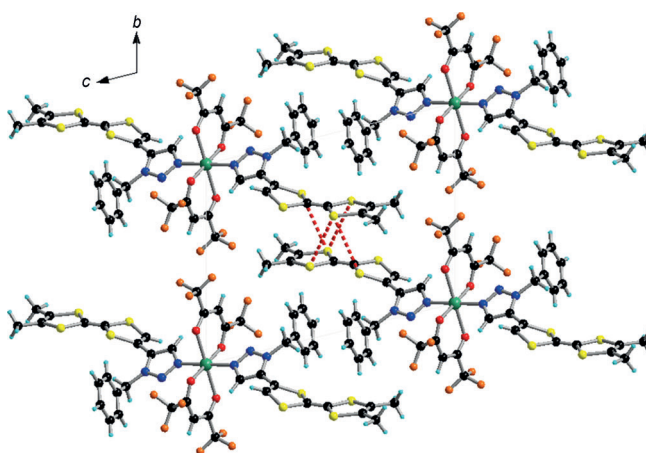


Figure 7. Packing diagram for **4b** in the *bc* plane. Intermolecular distances [Å]: $\text{S2}-\text{S2}$: 3.5, $\text{S2}-\text{S3}$: 3.89, $\text{S2}-\text{S1}$: 3.87, $\text{Cu}-\text{Cu}$: 7.25. Highlighted: $\text{S2}-\text{S3}$ and $\text{S2}-\text{S1}$.

Complex **4a** also crystallizes in the triclinic system, space group $P\bar{1}$, and presents identical structural characteristics as **4b**, which includes moderate twists of 38 and 43° between the TTF and triazole units (see Figures S7–9 in the Supporting Information), intermolecular $\text{CH}_{\text{TTF}} \cdots \text{O}_{\text{hfac}}$ and intramolecular $\text{CH}_{(\text{triazole})} \cdots \text{O}_{(\text{hfac})}$ contacts. Note that complexes **4a,b** represent, to the best of our knowledge, the first structurally characterized Cu^{II} complexes with monodentate 1,2,3-triazole ligands. Interestingly, CV measurements show, besides the typical pair of reversible oxidation processes, that the TTF units in **4a,b** oxidize at much lower potentials than in the free ligands **3a,b**, according to the $E^{1/2} = +0.28$ and $+0.23$ V, respectively, relative to $E^{1/2} = +0.49$ and $+0.44$ V in **3a,b**, which represents an important cathodic shift. The same trend is observed for the second oxidation process. This feature is in sharp contrast with the classical behavior of other TTF-based ligands, for which anodic shifts or unchanged potentials are observed for the TTF units upon complexation to a metal center.^[2] The unusual low-oxidation values observed here can be tentatively attributed to a more

efficient conjugation of the sp^3 N atom with the unsaturated system, as suggested by the comparatively shorter N3–C7, N3–N2, and N1–C8 bond lengths in **4a,b** relative to **3a,b**, which pushes some of the π electron density toward the TTF unit. Thus, it seems that the attachment of the $\{Cu(hfac)_2\}$ fragment on the triazole induces an electron enrichment of the TTF unit when compared to the ligand alone. It should be pointed out that, although in the solid state the TTF and triazole units are mutually twisted, which is the consequence of intermolecular hydrogen bonding (see above) that should not be operative in solution, and thus a coplanar arrangement might become the most stable conformation in the absence of packing forces and intermolecular interactions. To explain this unusual cathodic shift, one might also consider the involvement of the H_{TTF} or $H_{triazole}$ atoms (the distance $H8\cdots O2$ is only 2.69 Å in **4b** and on the same order of magnitude in **4a**) in intramolecular hydrogen bonding with the strongly negative fluorine or oxygen atoms of the hfac ligands, in line with the intermolecular $H5\cdots O1$ and intramolecular $H8\cdots O2$ interactions observed in the solid state. However, it seems more likely, with regard to the closer proximity of the triazole and hfac groups than TTF and hfac, that the main interaction should be $CH_{(triazole)}\cdots O_{(hfac)}$ as already observed in the solid state. Such an interaction, thus leading to a $C^{\delta-}-H^{\delta+}$ polarization, would produce an increase of electron density on the triazole ring and provide a partial triazolyl anion character, which is also supported by the shorter bond lengths within the ring in **4a, b** relative to the corresponding ligands **3a, b** (see above). Thus, the electron-enriched triazole ring would act as an electron-donating group toward TTF, and hence easier oxidation for the latter. In the UV/Vis spectrum of **4a** and **4b** the charge-transfer bands appear at $\lambda_{max}=403$ and 394 nm, respectively, with an intensity that is comparatively higher per TTF–triazole unit by a factor of 1.3, as indicated by $\epsilon=2010, 5220, 1760,$ and $4750\text{ M}^{-1}\text{ cm}^{-1}$ for **3a, 4a, 3b,** and **4b**, respectively.

Conclusion

We have synthesized two unprecedented families of monodentate TTF–1,2,3-triazole ligands as 1,4- and 1,5-isomers by using CuAAC and RuAAC click strategies, with a direct connection between the TTF unit and triazole ring. Their electrochemical and spectroscopic properties have been determined, compared, and supported by DFT calculations. Both series of compounds are excellent electron donors. The charge transfer from the TTF to the triazole unit can be possibly modulated by reaction with electrophiles, thus providing triazolium salts.^[21] The 1,5-isomers have been used to synthesize Cu^{II} complexes, which were structurally characterized and shown to be valuable precursors for paramagnetic molecular conductors. These two synthetic strategies can be extended to the preparation of TTF-based chelating pyridine–triazole ligands by the appropriate choice of the starting azide.^[22]

Experimental Section

General: Dry THF and diethyl ether were obtained from a solvent purification system (LC Technology Solutions Inc.). NMR spectra were recorded on a Bruker Avance DRX 300 spectrometer operating at 300 and 75 MHz for 1H and ^{13}C , respectively. The chemical shifts are expressed in parts per million (ppm, δ) downfield from external TMS. The following abbreviations are used: s=singlet, d=doublet, t=triplet, and m=multiplet. MALDI-TOF MS spectra were recorded on a Bruker Biflex-IIIITM apparatus equipped with a N_2 laser at $\delta=337$ nm. Elemental analyses were recorded using Flash 2000 Fisher Scientific Thermo Electron analyzer. IR spectra were recorded on Bruker FTIR Vertex 70 spectrometer equipped with a platinum–diamond ATR accessory. 2-Trimethylsilylethynyltetrathiafulvalene (**1a**) was prepared by using a reported procedure.^[23]

2-Ethynyl-tetrathiafulvalene 1a: Tetrabutylammonium fluoride (1.4 mL, 1.40 mmol; 1 M solution in THF) was added to a degassed solution of **1a** (350 mg, 1.17 mmol) in THF/methanol (30 mL, 1:1 v/v). The reaction mixture was stirred at room temperature for 45 min and then the solvents were removed under vacuum. The crude product was purified by flash chromatography over neutral alumina (CH_2Cl_2 as the eluent) to yield **1a** as an orange–brown oil (189 mg, 71%), which was directly engaged in the next step because of fast degradation. 1H NMR ($CDCl_3$, 300 MHz): $\delta=6.61$ (s, 1H), 6.44 (s, 2H), 3.27 ppm (s, 1H).

1-Benzyl-4-tetrathiafulvalenyl-1,2,3-triazole (2a): In a Schlenk tube, **1a** (150 mg, 0.66 mmol), benzyl azide (131 mg, 0.99 mmol), and CuI (7.5 mg, 6 mol%) were dissolved in $CHCl_3$ (5 mL) and *N,N*-diisopropylethylamine (3 mL). The reaction mixture was heated at 65°C overnight and concentrated under vacuum. The crude product was purified by chromatography over SiO_2 (CH_2Cl_2 /AcOEt (3:1) with a few drops of NEt_3 as the eluent; $R_f=0.3$) to yield **2a** as an orange–yellow solid (87 mg; 37%). Suitable single crystals for X-ray analysis were grown by vapor diffusion of pentane onto a solution of **2a** in CH_2Cl_2 . 1H NMR (CD_2Cl_2 , 300 MHz): $\delta=7.57$ (s, 1H), 7.47–7.41 (m, 3H), 7.37–7.32 (m, 2H), 6.78 (s, 1H), 6.41 (s, 2H), 5.58 ppm (s, 2H); [1H] ^{13}C NMR (CD_2Cl_2 , 75 MHz): $\delta=140.8, 134.6, 129.1, 128.8, 128.2, 125.0, 120.1, 119.2, 119.1, 115.0, 54.3$ ppm; MS (MALDI-TOF): m/z 361.0 [M^+]; elemental analysis (%) for $C_{15}H_{11}N_3S_4$: C 49.83, H 3.07, N 11.62, S 35.48; found: C 49.60, H 3.06, N 11.24, S 35.02.

1-Benzyl-5-tetrathiafulvalenyl-1,2,3-triazole (3a): In a Schlenk tube, **1a** (150 mg, 0.66 mmol), benzyl azide (131 mg, 0.99 mmol), and $[RuCp^*Cl(PPh_3)_2]$ (31 mg, 6 mol%) were dissolved in dry THF (8 mL). The reaction mixture was heated at 65°C overnight and concentrated under vacuum. The crude product was purified by chromatography over SiO_2 (CH_2Cl_2 /AcOEt (3:1) with a few drops of NEt_3 as the eluent; $R_f=0.3$) to yield **3a** as a dark-yellow oil, which rapidly solidifies (164 mg; 70%). Suitable single crystals for X-ray analysis were obtained by slow evaporation of solvent from a solution of **3a** in hexane/ CH_2Cl_2 . 1H NMR (CD_2Cl_2 , 300 MHz): $\delta=7.77$ (s, 1H), 7.44–7.35 (m, 3H), 7.24–7.18 (m, 2H), 6.42 (s, 2H), 6.30 (s, 1H), 5.69 ppm (s, 2H); [1H] ^{13}C NMR (CD_2Cl_2 , 75 MHz): $\delta=135.1, 134.4, 129.5, 129.0, 128.4, 127.1, 121.6, 119.4, 119.3, 119.2, 52.4$ ppm; MS (MALDI-TOF): m/z 360.6 [M^+]; elemental analysis (%) for $C_{15}H_{11}N_3S_4$: C 49.83, H 3.07, N 11.62, S 35.48; found: C 49.67, H 3.11, N 11.05, S 34.78.

2-Iodo-6,7-dimethyl-tetrathiafulvalene (o-DMTTF-I): In a Schlenk tube, 6,7-dimethyl-tetrathiafulvalene (*o*-DMTTF; 800 mg, 3.44 mmol) was dissolved in dry diethyl ether (100 mL) under argon at $-78^\circ C$. Diisopropylethylamine (532 μL , 3.79 mmol) followed by butyllithium (2.37 mL, 3.79 mmol; 1.6 M solution in hexane) were added to the reaction mixture, which was stirred at $-78^\circ C$ for 1 h and then a yellow precipitate appeared. Perfluorohexyl iodide (893 μL , 4.13 mmol) was added to the reaction mixture, which was allowed to warm slowly to room temperature and stirred overnight. After evaporation of the solvent, the crude product was purified by chromatography over SiO_2 (cyclohexane/ CS_2 (1:1) as the eluent; $R_f=0.8$) to yield *o*-DMTTF-I as a light-orange solid (790 mg, 64%). 1H NMR ($CDCl_3+NEt_3$, 300 MHz): $\delta=6.43$ (s, 1H), 1.98 ppm (s, 6H); [1H] ^{13}C NMR ($CDCl_3+NEt_3$, 75 MHz): $\delta=124.4, 122.9, 111.5, 110.1, 77.3, 13.8$ ppm; MS (MALDI-TOF): m/z 357.6 [M^+]; elemental

analysis (%) for C₈H₇IS₄: C 26.82, H 1.97, S 35.90; found: C 27.15, H 2.04, S 36.44.

2-Trimethylsilylethynyl-6,7-dimethyltetrafulvalene (1b): In a Schlenk tube, *o*-DMTTF-I (600 mg, 1.68 mmol), [Pd(PPh₃)₄] (97 mg, 5 mol%), and CuI (32 mg, 10 mol%) were dissolved in dry THF (15 mL). Diisopropylamine (1 mL, 7.12 mmol) and trimethylsilylacetylene (477 μL, 3.35 mmol) were added to the reaction mixture, which was heated at 60°C overnight under argon. After evaporation of the solvent, the crude product was purified by chromatography over SiO₂ (cyclohexane as the eluent; R_f=0.8) to yield **1b** as an orange solid (510 mg, 92%). ¹H NMR (CDCl₃+NEt₃, 300 MHz): δ=6.52 (s, 1H), 1.97 (s, 6H), 0.23 ppm (s, 9H); [¹H]¹³C NMR (CDCl₃+NEt₃, 75 MHz): δ=125.8, 123.0, 122.6, 116.0, 111.6, 107.1, 99.7, 95.2, 13.8, -0.3 ppm; MS (MALDI-TOF): *m/z* 327.7 [M⁺]; elemental analysis (%) for C₁₃H₁₄S₄Si: C 47.51, H 4.91, S 39.03 found: C 47.59, H 5.07, S 40.23.

2-Ethynyl-6,7-dimethyltetrafulvalene (1b): Tetrabutylammonium fluoride (1.1 mL, 1.11 mmol; 1 M solution in THF) was added to a degassed solution of **1b** (300 mg, 0.91 mmol) in THF/methanol (30 mL, 1:1 v/v). The reaction mixture was stirred at room temperature for 45 min and the solvents were removed under vacuum. The crude product was purified by flash chromatography over neutral alumina (CH₂Cl₂ as the eluent) to yield **1b** as an orange-brown solid (178 mg, 78%), which was directly engaged in the next step. ¹H NMR (CDCl₃, 300 MHz): δ=6.59 (s, 1H), 3.24 (s, 1H), 1.97 ppm (s, 6H).

1-Benzyl-4-(6',7'-dimethyltetrafulvalenyl)-1,2,3-triazole (2b): In a Schlenk tube, **1b** (150 mg, 0.59 mmol), benzyl azide (117 mg, 0.88 mmol), and CuI (6.7 mg, 6 mol%) were dissolved in CHCl₃ (5 mL) and *N,N*-diisopropylethylamine (3 mL). The reaction mixture was heated at 65°C overnight and concentrated under vacuum. The crude product was purified by chromatography over SiO₂ (CH₂Cl₂/AcOEt (3:1) with a few drops of NEt₃ as the eluent; R_f=0.3) to yield **2b** as a dark-yellow solid (102 mg, 45%). ¹H NMR (CDCl₃+NEt₃, 300 MHz): δ=7.44–7.39 (m, 4H), 7.32–7.29 (m, 2H), 6.81 (s, 1H), 5.55 (s, 2H), 1.98 ppm (s, 6H); [¹H]¹³C NMR (CDCl₃+NEt₃, 75 MHz): δ=141.3, 134.2, 129.3, 129.0, 128.2, 124.5, 122.9, 122.8, 119.9, 115.5, 54.6, 13.8 ppm; MS (MALDI-TOF): *m/z* 389.1 [M⁺]; elemental analysis (%) for C₁₇H₁₅N₃S₄: C 52.41, H 3.88, N 10.79, S 32.92; found: C 52.82, H 3.80, N 10.55, S 33.31.

1-Benzyl-5-(6',7'-dimethyl-tetrafulvalenyl)-1,2,3-triazole (3b): In a Schlenk tube, **1b** (150 mg, 0.59 mmol), benzyl azide (117 mg, 0.88 mmol), and [RuCp*Cl(PPh₃)₂] (28 mg, 6 mol%) were dissolved in dry THF (8 mL). The reaction mixture was heated at 65°C overnight and concentrated under vacuum. The crude product was purified by chromatography over SiO₂ (CH₂Cl₂/AcOEt (3:1) as the eluent; R_f=0.3) to yield **3b** as an orange-red solid (164 mg; 72%). Suitable single crystals for X-ray analysis were obtained by slow evaporation of solvent from a solution of **3b** in CH₂Cl₂. ¹H NMR (CDCl₃+NEt₃, 300 MHz): δ=7.76 (s, 1H), 7.38–7.35 (m, 3H), 7.21–7.18 (m, 2H), 6.17 (s, 1H), 5.67 (s, 2H), 2.00 ppm (s, 6H); [¹H]¹³C NMR (CDCl₃+NEt₃, 75 MHz): δ=134.8, 134.6, 129.6, 129.1, 128.5, 127.1, 123.0, 122.9, 121.6, 119.4, 52.5, 13.8 ppm; MS (MALDI-TOF): *m/z* 388.8 [M⁺]; elemental analysis (%) for C₁₇H₁₅N₃S₄: C 52.41, H 3.88, N 10.79, S 32.92; found: C 52.39, H 3.92, N 9.84, S 33.02.

4a: In a Schlenk tube, **3a** (14.5 mg, 0.04 mmol) and [Cu(hfac)₂]*x*H₂O (9.58 mg, 0.02 mmol) were stirred at 60°C in hexane/dichloromethane (8 mL, 1:1) over 1 h. The solution was allowed to return to room temperature, and dark-yellow crystals of **4a** were obtained after slow evaporation of the solvents (23 mg, 96%). MS (ES): *m/z* 994.77 [M-hfac⁺]; elemental analysis (%) for C₄₀H₂₆CuF₁₂N₆O₄S₈: C 39.95, H 2.18, N 6.99, S 21.33; found: C 39.77, H 2.24, N 6.62, S 21.58.

4b: In a Schlenk tube, **3b** (15.7 mg, 0.04 mmol) and [Cu(hfac)₂]*x*H₂O (10 mg, 0.02 mmol) were stirred at 60°C in hexane/dichloromethane (8 mL, 1:1) over 1 h. The solution was allowed to return to room temperature, and dark-yellow crystals of **4b** were obtained after slow evaporation of the solvents (25 mg, 98%). MS (ES): *m/z* 1050.87 [M-hfac⁺]; elemental analysis (%) for C₄₄H₃₄CuF₁₂N₆O₄S₈: C 41.98, H 2.72, N 6.68, S 20.38; found: C 41.87, H 2.75, N 6.44, S 20.82.

X-ray structure determinations: Details about data collection and solution refinement are given in Tables 2 and 3. X-ray diffraction measurements were performed on a Bruker Kappa CCD diffractometer operating

Table 2. Crystal data and structure refinement for the ligands **2a**, **3a**, and **3b**.

	2a	3a	3b
Empirical formula	C ₁₅ H ₁₁ N ₃ S ₄	C ₁₅ H ₁₁ N ₃ S ₄	C ₁₇ H ₁₅ N ₃ S ₄
FW	361.51	361.51	389.58
<i>T</i> [K]	293(2)	293(2)	293(2)
Crystal system	triclinic	orthorhombic	triclinic
Space group	<i>P</i> -1	<i>Pcab</i>	<i>P</i> -1
<i>a</i> [Å]	6.2917 (2)	7.7058 (6)	6.655 (3)
<i>b</i> [Å]	11.3734 (5)	19.852 (3)	9.5467 (17)
<i>c</i> [Å]	11.4902 (8)	20.971 (3)	14.134 (3)
α [°]	98.724 (5)	90.00	84.081 (15)
β [°]	96.622 (4)	90.00	84.93 (2)
γ [°]	101.683 (3)	90.00	78.43 (3)
<i>V</i> [Å ³]	786.76 (7)	3208.0 (7)	872.9 (5)
<i>Z</i>	2	8	2
<i>D</i> _c [g cm ⁻³]	1.526	1.497	1.482
Absorption coefficient [mm ⁻¹]	0.601	0.590	0.548
GOF on <i>F</i> ²	1.023	1.114	1.047
Final <i>R</i> indices [<i>I</i> >2σ(<i>I</i>)]	<i>R</i> 1=0.0438, <i>wR</i> 2=0.0757	<i>R</i> 1=0.0523, <i>wR</i> 2=0.0767	<i>R</i> 1=0.0494, <i>wR</i> 2=0.1108
<i>R</i> indices (all data)	<i>R</i> 1=0.0924, <i>wR</i> 2=0.0898	<i>R</i> 1=0.1190, <i>wR</i> 2=0.0929	<i>R</i> 1=0.0925, <i>wR</i> 2=0.1303

Table 3. Crystal data and structure refinement for the complexes **4a** and **4b**.

	C ₄₀ H ₂₆ CuF ₁₂ N ₆ O ₄ S ₈	C ₄₄ H ₃₄ CuF ₁₂ N ₆ O ₄ S ₈
Empirical formula	C ₄₀ H ₂₆ CuF ₁₂ N ₆ O ₄ S ₈	C ₄₄ H ₃₄ CuF ₁₂ N ₆ O ₄ S ₈
FW	1200.72	1256.78
<i>T</i> [K]	293(2)	293(2)
Crystal system	triclinic	triclinic
Space group	<i>P</i> -1	<i>P</i> -1
<i>a</i> [Å]	12.6740 (9)	7.2569 (6)
<i>b</i> [Å]	15.2920 (13)	12.2100 (18)
<i>c</i> [Å]	15.5360 (11)	15.479 (3)
α [°]	110.600 (7)	103.560 (12)
β [°]	100.420 (6)	90.642 (7)
γ [°]	111.11 (6)	98.604 (11)
<i>V</i> [Å ³]	2460.9 (3)	1316.8 (3)
<i>Z</i>	2	1
<i>D</i> _c [g cm ⁻³]	1.620	1.585
Absorption coefficient [mm ⁻¹]	0.876	0.822
GOF on <i>F</i> ²	1.004	1.058
Final <i>R</i> indices [<i>I</i> >2σ(<i>I</i>)]	<i>R</i> 1=0.0711, <i>wR</i> 2=0.1327	<i>R</i> 1=0.0461, <i>wR</i> 2=0.0888
<i>R</i> indices (all data)	<i>R</i> 1=0.2118, <i>wR</i> 2=0.1740	<i>R</i> 1=0.0831, <i>wR</i> 2=0.1030

with a MoKα (λ=0.71073 Å) X-ray tube with a graphite monochromator. The structures were solved (SHELXS-97) by direct methods and refined (SHELXL-97) by full-matrix least-square procedures on *F*². All non-hydrogen atoms were refined anisotropically. Hydrogen atoms were introduced at calculated positions (riding model), included in structure-factor calculations but not refined.

CCDC 875364 (**2a**), CCDC 875365 (**3a**), CCDC 875366 (**3b**), CCDC 894407 (**4a**), and CCDC 875367 (**4b**) contain the supplementary crystallographic data for this paper. These data can be obtained free of charge from The Cambridge Crystallographic Data Center via www.ccdc.cam.ac.uk/data_request/cif.

Electrochemical studies: CV measurements were performed by means of a three-electrode cell equipped with a platinum millielectrode with a surface area of 0.126 cm², an Ag/Ag⁺ pseudoreference, and a platinum-wire counterelectrode. The potential values were readjusted with respect to

the SCE. The electrolytic media involved a 0.1 mol L⁻¹ solution of (nBu)₄NPF₆ in CH₂Cl₂/CH₃CN (1:1). All the experiments were performed at room temperature at 0.1 V s⁻¹. Experiments were carried out with an EGG PAR 273A potentiostat with positive feedback compensation.

Theoretical calculations: Optimized geometries, starting from the X-ray data, were obtained with the Gaussian 09 package at the DFT level of theory (see the Supporting Information). The PBE0 functional^[24] was used. Vibrations frequency calculations performed on the optimized structures at the same level of theory yielded only positive values. TD-DFT calculations for the first 50 singlet excited states were performed at the same level of theory on the equilibrium geometries.

Acknowledgements

This work was supported by the CNRS, University of Angers, and the Ministry of Education and Research (grant to T.B.). I. Freuze and C. Mézière are thanked for the mass-spectrometric analyses.

- [1] a) J. L. Segura, N. Martin, *Angew. Chem.* **2001**, *113*, 1416; *Angew. Chem. Int. Ed.* **2001**, *40*, 1372; b) D. Canevet, M. Sallé, G. Zhang, D. Zhang, D. Zhu, *Chem. Commun.* **2009**, 2245.
- [2] a) D. Lorcy, N. Bellec, M. Fourmigué, N. Avarvari, *Coord. Chem. Rev.* **2009**, *253*, 1398; b) M. Shatruk, L. Ray, *Dalton Trans.* **2010**, *39*, 11105.
- [3] a) E. Coronado, P. Day, *Chem. Rev.* **2004**, *104*, 5419; b) L. Ouahab, T. Enoki, *Eur. J. Inorg. Chem.* **2004**, 933; c) F. Riobé, N. Avarvari, *Coord. Chem. Rev.* **2010**, *254*, 1523.
- [4] For selected references, see: a) F. Iwahori, S. Golhen, L. Ouahab, R. Carlier, J.-P. Sutter, *Inorg. Chem.* **2001**, *40*, 6541; b) C. Goze, C. Leiggener, S.-X. Liu, L. Sanguinet, E. Levillain, A. Hauser, S. Decurtins, *ChemPhysChem* **2007**, *8*, 1504; c) T. Devic, N. Avarvari, P. Batail, *Chem. Eur. J.* **2004**, *10*, 3697.
- [5] W. Liu, J. Xiong, Y. Wang, X.-H. Zhou, R. Wang, J.-L. Zuo, X.-Z. You, *Organometallics* **2009**, *28*, 755.
- [6] M. Nihei, N. Takahashi, H. Nishikawa, H. Oshio, *Dalton Trans.* **2011**, *40*, 2154.
- [7] T. Murata, Y. Morita, K. Fukui, K. Sato, D. Shiomi, T. Takui, M. Maesato, H. Yamochi, G. Saito, K. Nakasuji, *Angew. Chem.* **2004**, *116*, 6503; *Angew. Chem. Int. Ed.* **2004**, *43*, 6343.
- [8] J. Wu, N. Dupont, S.-X. Liu, A. Neels, A. Hauser, S. Decurtins, *Chem. Asian J.* **2009**, *4*, 392.
- [9] a) H. C. Kolb, M. G. Finn, K. B. Sharpless, *Angew. Chem.* **2001**, *113*, 2056; *Angew. Chem. Int. Ed.* **2001**, *40*, 2004; b) J. E. Moses, A. D. Moorhouse, *Chem. Soc. Rev.* **2007**, *36*, 1249.
- [10] a) V. V. Rostovtsev, L. G. Green, V. V. Fokin, K. B. Sharpless, *Angew. Chem.* **2002**, *114*, 2708; *Angew. Chem. Int. Ed.* **2002**, *41*, 2596; b) C. W. Tornøe, C. Christensen, M. Meldal, *J. Org. Chem.* **2002**, *67*, 3057; c) J. E. Hein, V. V. Fokin, *Chem. Soc. Rev.* **2010**, *39*, 1302.
- [11] a) Y.-L. Zhao, W. R. Dichtel, A. Trabolsi, S. Saha, I. Aprahamian, J. F. Stoddart, *J. Am. Chem. Soc.* **2008**, *130*, 11294; b) K. Qvortrup, M. Å. Petersen, T. Hassenkam, M. B. Nielsen, *Tetrahedron Lett.* **2009**, *50*, 5613.
- [12] a) L. Zhang, X. Chen, P. Xue, H. H. Y. Sun, I. D. Williams, K. B. Sharpless, V. V. Fokin, G. Jia, *J. Am. Chem. Soc.* **2005**, *127*, 15998; b) B. C. Boren, S. Narayan, L. K. Rasmussen, L. Zhang, H. Zhao, Z. Lin, G. Jia, V. V. Fokin, *J. Am. Chem. Soc.* **2008**, *130*, 8923.
- [13] A. C. Tomé in *Science of Synthesis: Houben-Weyl Methods of Molecular Transformations, Vol. 13* (Eds.: R. C. Storr, T. L. Gilchrist), Thieme, Stuttgart, **2004**, p. 415.
- [14] R. Bronisz, *Inorg. Chem.* **2005**, *44*, 4463.
- [15] a) B. M. J. M. Suijkerbuijk, B. N. H. Aerts, H. P. Dijkstra, M. Lutz, A. L. Spek, G. van Koten, R. J. M. K. Gebbink, *Dalton Trans.* **2007**, 1273; b) M. L. Gower, J. D. Crowley, *Dalton Trans.* **2010**, *39*, 2371; c) J. D. Crowley, E. L. Gavey, *Dalton Trans.* **2010**, *39*, 4035; d) H. Struthers, T. L. Mindt, R. Schibli, *Dalton Trans.* **2010**, *39*, 675.
- [16] D. S. Pedersen, A. Abell, *Eur. J. Org. Chem.* **2011**, 2399.
- [17] Y. H. Lau, P. J. Rutledge, M. Watkinson, M. H. Todd, *Chem. Soc. Rev.* **2011**, *40*, 2848.
- [18] G. Gasser, N. Hüsken, S. D. Köster, N. Metzler-Nolte, *Chem. Commun.* **2008**, 3675.
- [19] E. Chardon, G. L. Puleo, G. Dahm, G. Guichard, S. Bellemin-Lapponnaz, *Chem. Commun.* **2011**, *47*, 5864.
- [20] a) P. R. Ashton, V. Balzani, J. Becher, A. Credi, M. C. T. Fyfe, G. Matteredsteig, S. Menzer, M. B. Nielsen, F. M. Raymo, J. F. Stoddart, M. Venturi, D. J. Williams, *J. Am. Chem. Soc.* **1999**, *121*, 3951; b) R. Pou-Amérgigo, E. Ortí, M. Merchán, M. Rubio, P. M. Viruela, *J. Phys. Chem. A* **2002**, *106*, 631.
- [21] K. J. Kilpin, U. S. D. Paul, A.-L. Lee, J. D. Crowley, *Chem. Commun.* **2011**, *47*, 328.
- [22] a) J. D. Crowley, P. H. Bandeen, L. R. Hanton, *Polyhedron* **2010**, *29*, 70; b) P. M. Guha, H. Phan, J. S. Kinyon, W. S. Brotherton, K. Sreenath, J. T. Simmons, Z. Wang, R. J. Clark, N. S. Dalal, M. Shatruk, L. Zhu, *Inorg. Chem.* **2012**, *51*, 3465.
- [23] C. Goze, S.-X. Liu, C. Leiggener, L. Sanguinet, E. Levillain, A. Hauser, S. Decurtins, *Tetrahedron* **2008**, *64*, 1345.
- [24] C. Adamo, V. Barone, *J. Chem. Phys.* **1999**, *110*, 6158.

Received: May 30, 2012

Revised: August 29, 2012

Published online: October 18, 2012